Online Phase Noise Estimation in Structured Illumination Measurement Systems

Marc Fischer#, Marcus Petz and Rainer Tutsch

Technische Universität Braunschweig, Institut für Produktionsmesstechnik, Schleinitzstraße 20, 38106 Braunschweig, Germany
Corresponding Author / E-mail: marc.fischer@tu-braunschweig.de, TEL: +49-531-391-7023, FAX: +49-531-391-5837

KEYWORDS : Structured Illumination, Fringe Projection, Deflectometry, EMVA 1288, Phase Noise

In every measurement application it is generally desirable to get an estimate for the uncertainty in addition to the measured value. For structured illumination measurement systems, the calculated phase values are typically further processed into points in 3D-space by triangulation, and a geometrical primitive is then fitted to the point cloud. Without knowledge of phase noise, the points must be equally weighted, which induces systematic errors. The majority of prior research work concerning phase noise has been done in the field of interferometry. The results are most often based on the assumption of signal independent Gaussian noise. As modern cameras are typically limited by signal-dependent photon noise, strong deviations from this theory can be observed for high irradiations. In this paper, an approach that is based on the camera model of the standard EMVA 1288 is presented that takes this into account. It was possible to derive a formula that can be used to estimate the phase noise for each measurement point directly from the recorded digital gray values and parameters that can be found in an EMVA 1288 compliant datasheet. The findings are validated by means of simulations and experiments.

Manuscript received: January XX, 2011 / Accepted: January XX, 2011

NOMENCLATURE

M = number of phase-shifted images
I = intensity
I′ = unmodulated intensity
I″ = modulation
φ = phase angle
ψ = phase-shift
γ = relative modulation (visibility)
β = relative unmodulated intensity (illumination)
N = nominator of a phase-shift algorithm
D = denominator of a phase-shift algorithm
ρ = correlation coefficient
α = magnitude ratio
η = total quantum efficiency
K = overall system gain
n = number of elements (electrons or photons)
μ = expectation value
σ = standard deviation
y = output digital gray value
SNR = signal-to-noise ratio

Subscripts:
i – refers to the i-th phase-shifted image
e – refers to electrons
p – refers to photons
d – refers to dark noise
q – refers to quantization noise
sat – refers to the saturation limit
est – refers to estimated values

1. Introduction

The basis for several optical measurement techniques is the calculation of a phase value from multiple phase-shifted sinusoidal signals. In phase-shifting interferometry, for example, the interference fringes for each phase-shift are recorded with a camera and the phase value resulting per pixel can be directly transferred into the optical path difference or the surface height respectively. Huge effort has been made in the last decades to derive algorithms for phase evaluation that are able to suppress the systematic errors that typically influence an interferometric measurement, such as phase-shift errors, vibrations or non-sinusoidal signals. An extensive systematic overview of the numerous algorithms can be found in [1]. As systematic effects typically dominate stochastic influences in interferometry, only few authors considered phase noise and most often assumed signal-independent

Gaussian noise [2][3][4].

Besides interferometry, the phase-shifting approach is also used with incoherent light in structured illumination measurement systems. In these systems the phase-shifted fringe patterns are projected onto the object (fringe projection) or displayed on a screen (deflectometry). The sensitivity to vibrations is inherently much smaller than in interferometry and as long as the phase-shifted images are displayed on a digital device like a projector (DLP) or a monitor (LCD), the phase-shift error is limited by the manufacturing accuracy of the pixel structure. In this case one of the main systematic error sources for phase evaluation is the aliasing effect caused by the discrete pixel structure, both in the light emitter and the detector. As this effect can be significantly reduced by defocusing [5], it is possible to decrease systematic errors to the order of magnitude of stochastic errors. Thus phase noise, resulting from statistical variations of the recorded intensities, is by far more important in structured illumination systems than in interferometric systems.

In contrast to the assumption of signal-independent Gaussian noise, modern scientific and industrial cameras tend to be limited by Poisson-distributed photon noise that increases with signal strength. The European Machine Vision Association has published a standard for general camera and image sensor characterization that takes this into account. The "EMVA Standard 1288 – Standard for Characterization of Image Sensors and Cameras" (EMVA 1288) [6] is based on an advanced linear camera model that incorporates normal-distributed electronic noise, Poisson-distributed photon noise and quantization noise. The updated release 3.0 has been published in November 2010. It is meant to be a guideline for manufacturers to generate comparable datasheets and for customers to correctly interpret these EMVA 1288 compliant specifications. The fundamental camera model of the EMVA 1288 has already been successfully applied to accuracy analysis of measurement systems by Bothe [7] for a fringe projection system and by Erz [8] for a time-of-flight measurement system.

In every measurement application it is generally desirable to get an estimate for the uncertainty in addition to the measured value. This is most often done by evaluating repeated measurements. For structured illumination measurement systems this is usually not really practical because of constrained measurement time, especially in industrial applications. In these systems the calculated phase values are typically further processed into points in 3D-space by triangulation. In the last step usually a geometrical primitive is fitted to the point cloud. As there is no uncertainty information available, the points are equally weighted for the fitting process, which induces systematic errors because the significance of points resulting from phase values with high noise is overestimated. As a solution, the fringe contrast is sometimes used as the basis for a quality indicator [1], which again is only valid for the assumption of signal-independent Gaussian noise and leads to systematic errors in the presence of Poisson-distributed photon noise.

In this paper, a model for phase noise is described that is based on the EMVA 1288 camera model. It is valid for linear image sensors in the presence of electronic, photon and quantization noise. The model is able to correctly predict the phase noise characteristic for a camera, defined by its parameters that can be found in an EMVA 1288 compliant datasheet. Additionally, a method for the online estimation of phase noise for each measurement point is derived. This method directly uses the recorded intensities together with the camera parameters to calculate an individual uncertainty estimation for each phase value.

2. Basic Concepts

2.1 Structured Illumination Measurement Systems

Optical measurement systems that use intensity patterns to spatially encode an object are referred to as "structured illumination" techniques. Among others, a widely applied coding approach is based on multiple phase-shifted sinusoidal fringe patterns. In this case the actual coding takes place in the time domain, as the phase-shifted patterns are usually recorded sequentially. Other methods, which can be based on binary patterns or Fourier analysis for example, are out of the scope of this paper.

The recorded intensity I_i for each pixel in the i-th phase-shifted image can be written as a sum of an unmodulated constant and a modulation term:

$$I_i = I' + I'' \cos(\varphi + \psi_i); \quad i = 1,...,M \tag{1}$$

where I' is the unmodulated intensity, I'' the signal modulation, φ the unknown phase angle, ψ_i the applied phase-shift and M the number of phase-shifted images. For a general discussion it is useful to eliminate the absolute reference of I' and I''. By defining:

$$I' = \beta I_{sat} \tag{2}$$

and

$$I'' = \gamma I' \tag{3}$$

it is possible to write (1) as:

$$I_i = I_{sat}\beta\left[1 + \gamma \cos(\varphi + \psi_i)\right] \tag{4}$$

where I_{sat} is the saturation intensity of the image sensor, β the relative unmodulated intensity (illumination) and γ the relative fringe contrast (visibility).

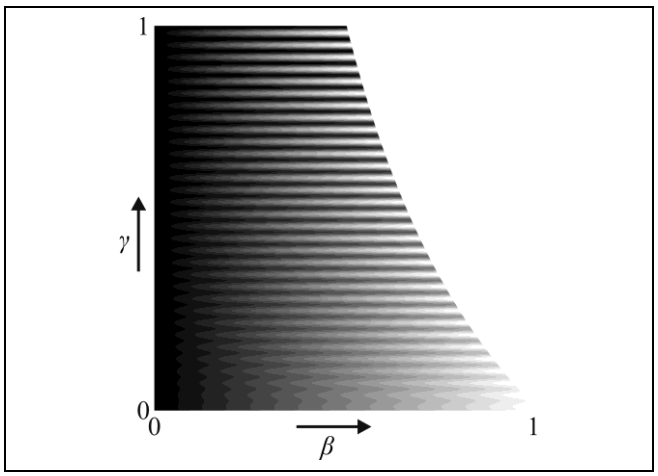

Fig. 1: Fringe pattern with locally varying visibility (γ) and illumination (β). In the right part of the diagram, points that do not meet the constraint for the maximum illumination (5) are painted white.

The advantage of this formulation is the separation of scaling from effects that only influence the fringe contrast. Furthermore (4) can be easily adapted to different intensity quantities, like number of photons or digital gray values, by choosing the appropriate value for I_{sat}, as the fundamental quantities β and γ are not affected by this. The value for β in a recorded image is mainly influenced by the maximum

brightness of the light emitting device and the aperture stop and exposure time setting of the camera. Additionally, also angle-dependent effects, like the reflectance characteristic of the object or the viewing angle of a display, affect the resulting β. The visibility γ on the other hand mainly depends on the maximum contrast of the projector or display, the modulation transfer function of the camera optics and the amount of residual light. Both parameters are in the range of [0…1] with an additional constraint of the maximum β for a given γ because I_i should always be smaller then I_{sat}:

$$\beta \le \frac{1}{1+\gamma} \tag{5}$$

The effect of β and γ on the recorded images can be visualized by means of a fringe pattern with locally varying visibility and illumination as demonstrated in Fig. 1. As can be seen the optimum fringe contrast can be achieved for $\beta = 0.5$ and $\gamma = 1$.

2.2 Phase-Shift Algorithms

With the recorded intensities I_i according to (4) the corresponding unknown phase value can be calculated by means of phase-shift algorithms. As mentioned above, most of the published algorithms address the reduction of systematic errors. In [2] a systematic investigation of the phase noise characteristic based on bivariate distribution functions has been carried out. Starting from a general formulation of a phase-shift algorithm with a nominator N and a denominator D that are functions of the recorded intensities:

$$\tan\varphi = \frac{N(I_1,\ldots,I_M)}{D(I_1,\ldots,I_M)} \tag{6}$$

it was shown that the general shape of the resulting distribution function for the phase angle φ, which can only be assumed Gaussian for high signal-to-noise ratios (SNR), mainly depends on two other parameters: the correlation coefficient ρ and the magnitude ratio α. With:

$$\rho = \frac{\sigma_{DN}}{\sigma_D \sigma_N} \tag{7}$$

and

$$\alpha = \frac{\sigma_N}{\sigma_D} \tag{8}$$

only for $\rho = 0$ and $\alpha = 1$ the distribution function of φ is phase-independent and the phase-shift algorithm is an unbiased estimator of the phase angle. Thus many of the algorithms proposed for interferometry are not suitable for structured illumination applications, which has also been concluded by Bothe in [7]. A class of algorithms that satisfy both conditions is based on evenly spaced phase-shifts over one period:

$$\tan\varphi = \frac{-\sum_{i=1}^{M} I_i \sin\psi_i}{\sum_{i=1}^{M} I_i \cos\psi_i}; \quad \psi_i = \frac{i2\pi}{M} \tag{9}$$

with the famous 4-step algorithm for M = 4:

$$\tan\varphi = \frac{I_3 - I_1}{I_4 - I_2}; \quad \psi_i = \left(\frac{\pi}{2}; \pi; \frac{3\pi}{2}; 2\pi\right) \tag{10}$$

For this class of phase-shift algorithms a simple expression for the phase-noise can be found according to [3] as:

$$\sigma_\varphi = \sqrt{\frac{2}{M}}\frac{1}{\gamma}\frac{\sigma_I}{I'} = \sqrt{\frac{2}{M}}\frac{1}{\gamma}\frac{1}{SNR} \tag{11}$$

Although this expression was based on the assumption of signal-independent Gaussian noise (σ_I = const.), where the signal-to-noise ratio would increase linearly with the unmodulated intensity I', in section 3 it is shown that it is also valid for the more complex expression of SNR resulting from the advanced linear camera model of the EMVA 1288.

2.3 EMVA 1288 Camera Model

In the following sections the linear camera model of the EMVA 1288 is briefly introduced. The standard describes measurement and evaluation procedures for temporal and spatial noise. Additionally, it also addresses temperature and exposure time dependent dark current noise. For the analysis in this paper only temporal noise is taken into account, as the phase evaluation does not depend on adjacent pixels and the exposure times are usually in an order of magnitude where the influence of dark current can be neglected.

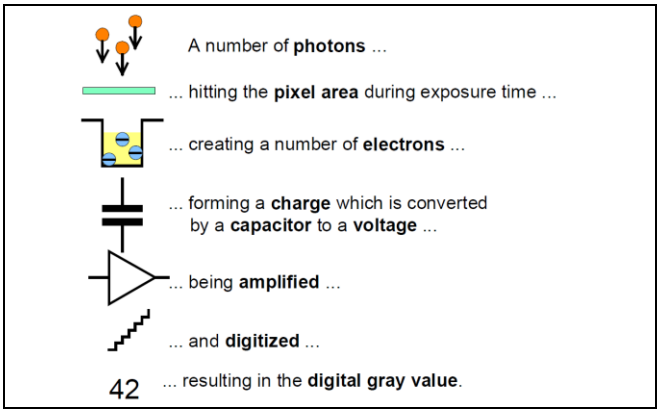

Fig. 2: Physical model of signal generation in a CCD-camera pixel according to EMVA 1288. Although the readout process differs slightly for CMOS-sensors, the same model can be used also in this case if the sensor can be assumed to be linear. [6]

The basic physical model of signal generation in a camera pixel is shown in Fig. 2, the resulting mathematical model in Fig. 3. It can be seen that the fundamental process is a conversion, first from number of photons n_p to number of electrons n_e with the total quantum efficiency η as the conversion factor and second to digital gray values with the system gain K as the conversion factor. Three noise sources are then added to the model with the following assumptions: the number of electrons n_e is Poisson-distributed ($\sigma_e^2 = \mu_e$), the number of dark noise electrons n_d is normally distributed (μ_d ; σ_d), and the quantization noise is uniformly distributed ($\sigma_q^2 = 1/12$).

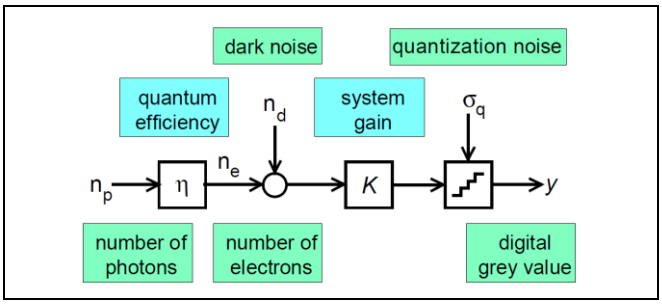

Fig. 3: Mathematical camera model according to EMVA 1288. The whole process is assumed to be linear. [6]

The variances of all noise sources can be added to result in the temporal variance of the output signal σ_y^2:

$$\sigma_y^2 = K^2\left(\sigma_e^2 + \sigma_d^2\right) + \sigma_q^2 \tag{12}$$

which is the basis for the definition of the SNR according to the EMVA 1288:

$$SNR = \frac{\mu_y - \mu_{y,d}}{\sigma_y} = \frac{\eta\mu_p}{\sqrt{\eta\mu_p + \sigma_d^2 + \frac{1}{12}\frac{1}{K^2}}} \tag{13}$$

It can be seen that the irradiation μ_p is also present in the expression for σ_y so that the magnitude of intensity noise is signal dependent. This function is approximately linear for small values of μ_p and changes gradually with increasing irradiation to a square root relationship. This can be easily recognized as the asymptotes of the example SNR-plot shown in Fig. 4.

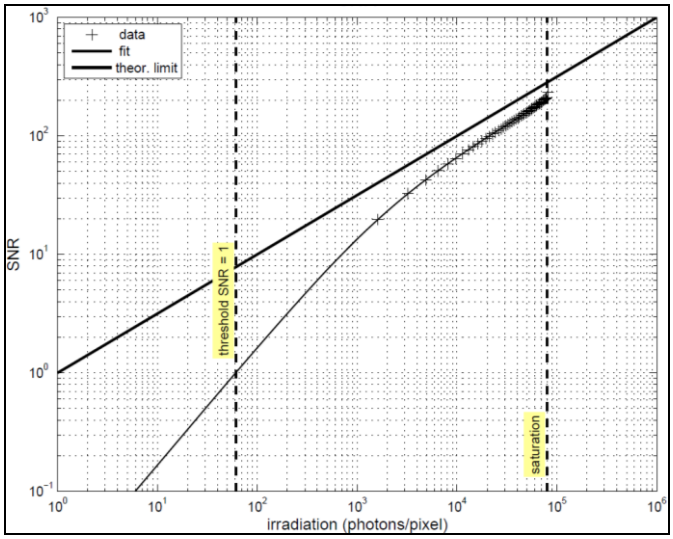

Fig. 4: Example of a SNR-plot that can be found in an EMVA 1288 compliant datasheet. The curve approximates a linear relationship for small irradiations (slope = 1) and a square root relationship for high irradiations (slope = 1/2) due to photon noise. [6]

3. Phase Noise Model based on EMVA 1288

An expression for the phase noise for the symmetrical M-step algorithm based on the advanced camera model of the EMVA 1288 can be derived by combining (11) and (13) and taking into account that according to Fig. 3 and (2) the illumination can be related to the electron saturation capacity $\mu_{e,sat}$ as:

$$\eta\mu_p = \mu_e = \beta\mu_{e,sat} \tag{14}$$

resulting in:

$$\sigma_\varphi = \sqrt{\frac{2}{M}}\frac{1}{\gamma\beta\mu_{e,sat}}\sqrt{\beta\mu_{e,sat} + \sigma_d^2 + \frac{1}{12K^2}} \tag{15}$$

In (15) all parameters are either determined by the measurement process (β, γ, M) or can be found in an EMVA 1288 compliant datasheet ($\mu_{e,sat}$, σ_d, K).

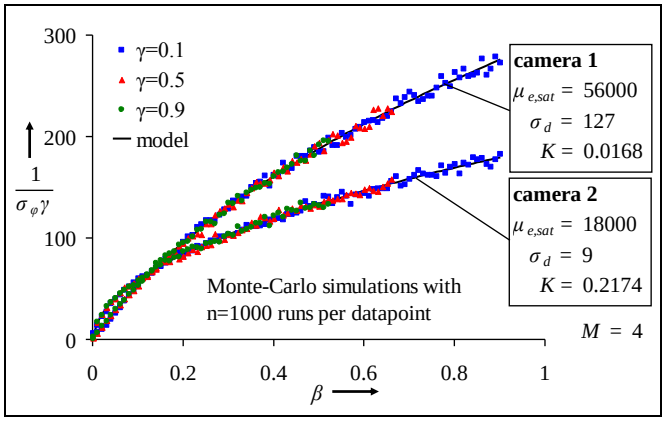

Fig. 5: Results of Monte-Carlo simulations to validate (15). For enhanced readability, the inverse of σ_φ divided by γ is plotted against β. This way all simulated combinations of β and γ are represented by the same model-curve.

Expression (15) has been validated by means of Monte-Carlo simulations (Fig. 5) and experiments (Fig. 6). For the experimental studies, a LCD-monitor was used to generate patterns with different combinations of β and γ and evaluating 1000 phase calculations. Systematic deviations are only evident for very small values of β and γ below 0.1, which is out of range for typical measurements with a structured illumination system.

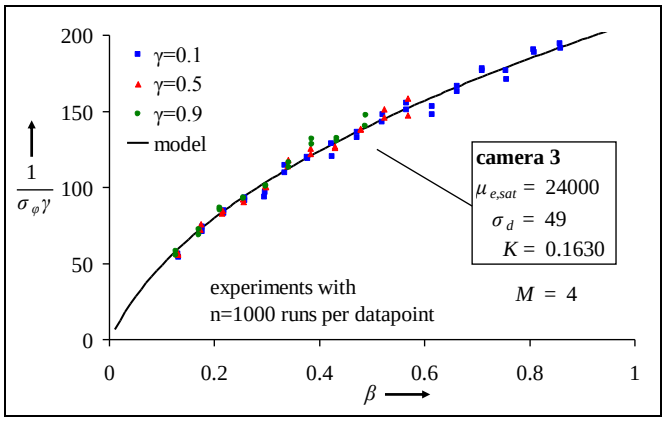

Fig. 6: Results of experiments to validate (15). For enhanced readability, the inverse of σ_φ divided by γ is plotted against β. This way all measured combinations of β and γ are represented by the same model-curve.

As can be seen, the phase noise model based on the EMVA 1288 is able to predict the phase evaluation precision of the symmetrical M-step algorithm with a given camera. The camera parameters can either be taken from an EMVA 1288 compliant datasheet, or derived experimentally with the methods described in the standard.

4. Online Estimation of Phase Noise

With the advanced phase noise model described in section 3 it is possible to compare the phase evaluation precision of different cameras for a specific measurement task. However it can not be used directly to assign uncertainty values to each measurement point, as the values for γ and β depend on the object that is measured. Thus a statistical evaluation over all measurement points is not reasonable. But it is possible to solve the set of equations (1) in addition to the phase angle φ also for I' and I'', resulting in expressions that depend on the measured intensities I_i. For the symmetrical M-step algorithm these can be found according to [1] as:

$$I' = \frac{1}{M}\sum_{i=1}^{M} I_i \tag{16}$$

and

$$I'' = \frac{2}{M}\sqrt{\left(\sum_{i=1}^{M} I_i \sin\psi_i\right)^2 + \left(\sum_{i=1}^{M} I_i \cos\psi_i\right)^2} \tag{17}$$

which can be combined with (2) and (3) to expressions for the estimated values β_{est} and γ_{est}:

$$\beta_{est} = \frac{I'}{I_{sat}} = \frac{\frac{1}{M}\sum_{i=1}^{M} I_i}{K\mu_{e,sat}} \tag{18}$$

and

$$\gamma_{est} = \frac{I''}{I'} = 2\frac{\sqrt{\left(\sum_{i=1}^{M} I_i \sin\psi_i\right)^2 + \left(\sum_{i=1}^{M} I_i \cos\psi_i\right)^2}}{\sum_{i=1}^{M} I_i} \tag{19}$$

As the measured intensities are noisy, also the estimated values vary statistically. This is demonstrated in Fig. 7, where each pair of β_{est} and γ_{est} for different combinations of the nominal values β and γ is represented by a small dot.

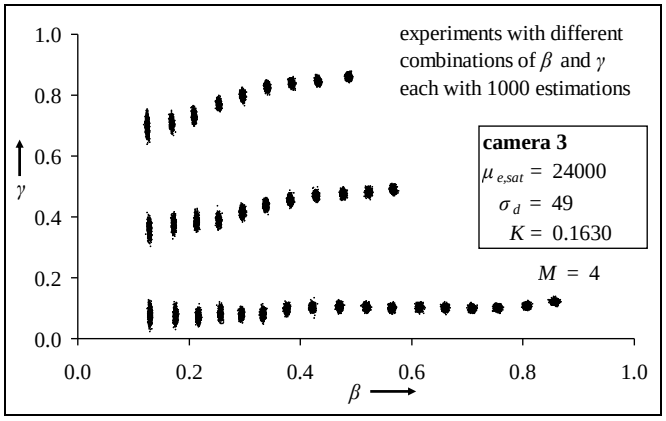

Fig. 7: Results of experiments to demonstrate the spread of the estimated values β_{est} and γ_{est}. Each dot represents an estimated value pair. The evaluation has been repeated for different combinations of the nominal values.

For the further investigation it has to be taken into account that the measured intensities I_i in (18) and (19) are not directly represented by the output gray values of the camera y_i, as the dark noise $\mu_{y,d}$ must be subtracted in advance according to (13). When this correction has been applied, (18) and (19) can be inserted into (15) and simplified to:

$$\sigma_{\varphi,est} = \sqrt{\frac{\frac{K}{2}\sum_{i=1}^{M} y_i + \frac{K^2 M}{2}\left(\sigma_d^2 - \mu_d\right) + \frac{M}{24}}{\left(\sum_{i=1}^{M} y_i \sin\psi_i\right)^2 + \left(\sum_{i=1}^{M} y_i \cos\psi_i\right)^2}} \tag{20}$$

This formula can be applied to estimate the phase evaluation precision of a measurement based on the symmetrical M-step algorithm directly from the output digital gray values and some camera parameters that can be found in an EMVA 1288 compliant datasheet. For the accuracy of this estimation it can be found that:

$$\sigma_{(\sigma_{\varphi,est})} = \sigma_\varphi^2 \tag{21}$$

which means that the relative error of the estimation equals the estimated phase noise. The findings have been validated by means of Monte-Carlo simulations and experiments. The results for the experiments are shown in Figs. 8 and 9.

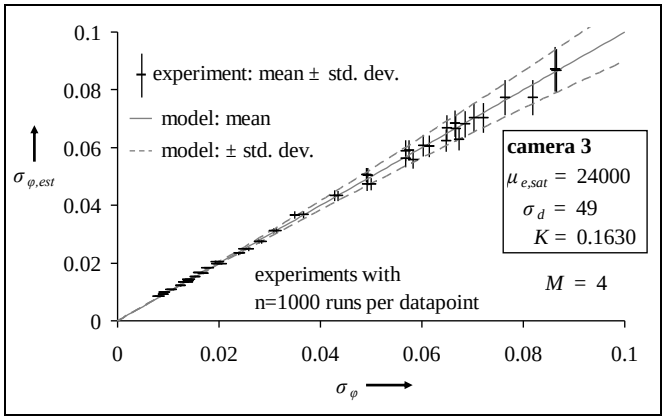

Fig. 8: Results of experiments to validate (20). The estimated phase noise $\sigma_{\varphi,est}$ has been plotted against the measured value σ_φ. The gray lines represent the expected spread of the estimation according to (21).

It can be seen that the proposed method is indeed able to estimate the phase noise for each measurement point. The relative error is < 6% for $\sigma_\varphi < 0.06$ which corresponds to a phase evaluation precision of about $\lambda/100$ as a typical range for structured illumination measurement systems.

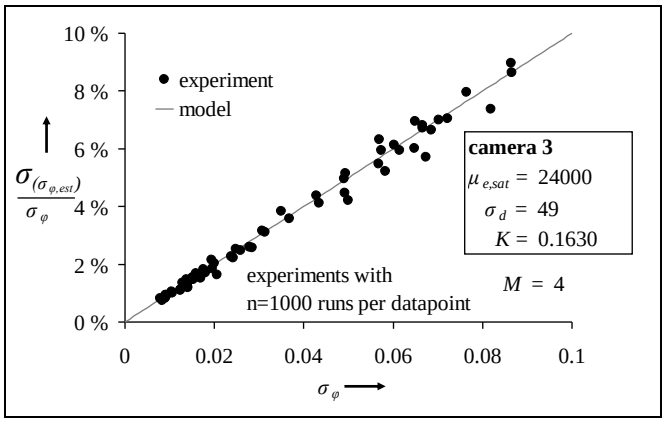

Fig. 9: Results of experiments to validate (21). The relative error of the estimation is plotted against the measured phase noise.

5. Conclusions

In this paper a method for the online estimation of phase noise in structured illumination measurement systems has been proposed. It is based on the advanced linear camera model of the EMVA 1288 which has been adapted to the characteristic image properties that are typical for this kind of application. It has been discussed that the symmetric M-step algorithm with evenly spaced phase-steps yields the best results in terms of phase noise, as it is an unbiased estimator without phase-dependent stochastic errors. For this algorithm an expression for the phase noise that depends on parameters given in an EMVA 1288 compliant datasheet could be derived. This has been further developed to an expression for the phase-noise that depends directly on the recorded digital gray values. This expression can be used to estimate the phase noise independently for each calculated phase value. The phase noise estimation can then be applied as a weight for subsequent data-processing like triangulation or fitting of geometrical primitives. All findings have been validated by means of Monte-Carlo simulations and experiments.

ACKNOWLEDGEMENT

The authors gratefully acknowledge the funding of this work by Deutsche Forschungsgemeinschaft (DFG) under grant Pe1402/2-1.

REFERENCES

1. Schreiber, H. and Bruning, J. H., “Phase Shifting Interferometry”, Malacara, D. (ed.), “Optical Shop Testing,” 3rd ed., Hoboken, NY: Wiley, pp. 547-655, 2007.
2. Rathjen, C., “Statistical properties of phase-shift algorithms,” Journal of the Optical Society of America A, Vol. 12, No. 9, pp. 1997-2008, 1995.
3. Surrel, Y., “Additive noise effect in digital phase detection,” Applied Optics, Vol. 36, No. 1, pp. 271-276, 1997.
4. Hibino, K., “Susceptibility of systematic error-compensating algorithms to random noise in phase-shifting interferometry,” Applied Optics. Vol. 36, No. 10, pp. 2084-2093, 1997.
5. Notni, G. H. and Notni, G., “Digital fringe projection in 3D shape measurement – an error analysis,” Osten, W., Kujawinska, M., Creath, K. (ed.), Proceedings of SPIE. 5144, Optical Measurement Systems for Industrial Inspection III, pp. 372-380, 2003.
6. European Machine Vision Association EMVA 1288, “Standard for Characterization of Image Sensors and Cameras,” Release 3.0, November 29th, 2010.
7. Bothe, T., “Grundlegende Untersuchung zur Formerfassung mit einem neuartigen Prinzip der Streifenprojektion und Realisierung in einer kompakten 3D-Kamera,“ PhD thesis, Vollertsen, F. and Bergmann, R. (ed.), Strahltechnik, Vol. 32, Bremen, BIAS Verlag, pp. 52-60, 2008.
8. Erz, M., “Charakterisierung von Laufzeitkamerasystemen für Lumineszenzlebensdauermessungen,“ PhD thesis, Heidelberg, Universität Heidelberg, pp. 58-62, 2011.